Autophagy Negatively Regulates Cell Death by Controlling NPR1-Dependent Salicylic Acid Signaling during Senescence and the Innate Immune Response in *Arabidopsis* [W][OA]

Kohki Yoshimoto,[a,1] Yusuke Jikumaru,[a] Yuji Kamiya,[a] Miyako Kusano,[a] Chiara Consonni,[b] Ralph Panstruga,[b] Yoshinori Ohsumi,[c,2] and Ken Shirasu[a]

[a] RIKEN, Plant Science Center, Tsurumi-ku, Yokohama 230-0045, Japan
[b] Max-Planck-Institute for Plant Breeding Research, Department of Plant–Microbe Interactions, D-50829 Koeln, Germany
[c] Department of Cell Biology, National Institute for Basic Biology, Myodaiji-cho, Okazaki 444-8585, Japan

Autophagy is an evolutionarily conserved intracellular process for vacuolar degradation of cytoplasmic components. In higher plants, autophagy defects result in early senescence and excessive immunity-related programmed cell death (PCD) irrespective of nutrient conditions; however, the mechanisms by which cells die in the absence of autophagy have been unclear. Here, we demonstrate a conserved requirement for salicylic acid (SA) signaling for these phenomena in autophagy-defective mutants (*atg* mutants). The *atg* mutant phenotypes of accelerated PCD in senescence and immunity are SA signaling dependent but do not require intact jasmonic acid or ethylene signaling pathways. Application of an SA agonist induces the senescence/cell death phenotype in SA-deficient *atg* mutants but not in *atg npr1* plants, suggesting that the cell death phenotypes in the *atg* mutants are dependent on the SA signal transducer NONEXPRESSOR OF PATHOGENESIS-RELATED GENES1. We also show that autophagy is induced by the SA agonist. These findings imply that plant autophagy operates a novel negative feedback loop modulating SA signaling to negatively regulate senescence and immunity-related PCD.

INTRODUCTION

Autophagy is an intracellular degradation process that delivers cytoplasmic constituents to the vacuole/lysosome (Klionsky and Ohsumi, 1999; Klionsky, 2005, 2007). During the autophagic event, bulk cytoplasmic constituents and organelles are engulfed into a double membrane vesicle called an autophagosome. The outer membrane of the autophagosome then fuses to the vacuolar membrane, delivering an inner membrane structure called an autophagic body, into the vacuolar lumen for degradation by resident hydrolases. The autophagy-mediated degradation process has been well elucidated at the molecular level in yeast (*Saccharomyces cerevisiae*). Genetic analyses in yeast identified 18 *autophagy-related* (*ATG*) genes that are essential for autophagosome formation (Tsukada and Ohsumi, 1993; Thumm et al., 1994; Barth et al., 2001). Most of the *ATG* genes are well conserved across plant and animal kingdoms, suggesting that the molecular basis of the core autophagy machinery is essentially the same in higher eukaryotes, although four out of 18 *ATG*

genes have not been identified in plants yet (Meijer et al., 2007). Indeed, *Arabidopsis thaliana ATG*-deficient mutants are defective in autophagy, confirming that ATG proteins are essential for plant autophagy (Bassham et al., 2006).
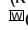
Arabidopsis atg mutants, such as *atg7-1* (Doelling et al., 2002), *atg9-1* (Hanaoka et al., 2002), *atg4a4b-1* (Yoshimoto et al., 2004), *atg5-1* (Thompson et al., 2005), *atg10-1* (Phillips et al., 2008), *ATG6*-RNA interference (RNAi; Patel and Dinesh-Kumar, 2008), and *ATG18a*-RNAi plants (Xiong et al., 2005) are all defective in autophagy but are able to complete normal embryogenesis, germination, cotyledon development, shoot and root elongation, flowering, and seed production under normal nutrient-rich conditions. These plants are, however, hypersensitive to nutrient-limiting conditions, and transcripts of some of the *ATG* genes are induced during starvation (Rose et al., 2006; van der Graaff et al., 2006; Chung et al., 2009). Recently, we found that chloroplast-derived ribulose-1,5-bisphosphate carboxylase/oxygenase–containing bodies and whole chloroplasts are delivered to the vacuole and degraded by autophagy under nutrient-limiting conditions (Ishida et al., 2008; Wada et al., 2009). Based on these data, plant autophagy has been proposed to play an important role mainly in nutrient recycling.
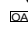
There are several lines of evidence that plant autophagy may also have other functions. For instance, ATG proteins are expressed even under nutrient-rich conditions (Doelling et al., 2002; Hanaoka et al., 2002; Yoshimoto et al., 2004; Thompson et al., 2005; Phillips et al., 2008; Chung et al., 2009). In nutrient-rich conditions, several *atg* mutants exhibit an early senescence phenotype (Doelling et al., 2002). In addition, autophagic defects

can cause excessive immunity-related programmed cell death (PCD), irrespective of nutrient conditions (Liu et al., 2005; Patel and Dinesh-Kumar, 2008). Silencing of *ATG6* in *Nicotiana benthamiana* resulted in reduced autophagy and spread of chlorotic cell death around the infection site after inoculation with *Tobacco mosaic virus* (TMV; Liu et al., 2005). This phenotype was not due to virus movement because transient expression of the elicitor protein (TMV-p50) alone was sufficient to induce the spread of chlorotic cell death in leaves of *ATG6*-silenced tobacco plants. A similar phenotype was also observed in *ATG6*-RNAi plants when infected with *Pseudomonas syringae* pv *tomato* bacteria DC3000 expressing *avrRpm1* (*Pst-avrRpm1*) (Patel and Dinesh-Kumar, 2008); however, mechanisms underlying this phenomenon have not been elucidated, and, thus, physiological roles of plant autophagy under nutrient-rich conditions have still remained elusive.

Here, we investigated the mechanism that induces early senescence and excessive immunity-related PCD in the autophagy-defective plants under nutrient-rich conditions. By biochemical analysis, we found that salicylic acid (SA) accumulated to high levels in the *atg2* and *atg5* mutants. The early senescence in *atg5* was suppressed by expressing *NahG*, which encodes an SA hydroxylase, to deplete endogenous SA, or by reducing SA biosynthesis using *sid2*, or by blocking SA signaling using *npr1*. The excessive immunity-related PCD in *atg5* was also suppressed in the *sid2* or *npr1* backgrounds, further confirming that these phenotypes are due to the failure of SA signaling control in the *atg* mutants. Application of an SA agonist, benzo(1,2,3) thiadiazole-7-carbothioic acid (BTH), restored the senescence/cell death phenotype in *NahG atg5* or *atg5 sid2* but not in *atg5 npr1* plants, and similar results were seen for *atg2*. These results reveal that autophagy operates a negative feedback loop modulating SA signaling and that this negative feedback limits senescence and immunity-related PCD in plants.

RESULTS

Autophagy-Defective Mutants Exhibit an Early Senescence Phenotype under Nutrient-Rich Conditions

To investigate the function of autophagy in nutrient-rich conditions, we analyzed *Arabidopsis atg* mutants in a rich soil. We found that *atg2* and *atg5* mutant plants, which completely lack autophagy, showed an early senescence phenotype even under favorable growth conditions (Figure 1A). As all other examined *atg* mutants, *atg4a4b*, *atg7*, *atg9*, *atg10*, and *atg18a*, exhibited a similar early senescence phenotype, we decided to use *atg2* and especially *atg5* mutants as a representative of autophagy-defective mutants for further experiments. The early senescence phenotype was observed under both long-day (16-h-light/8-h-dark cycles) and short-day (8-h-light/16-h-dark cycles) conditions (Figure 1B). Under the long-day condition, the first and second leaves started to turn yellow from the edge at around week 4 in *atg2* and week 5 in *atg5*, respectively. By contrast, in wild-type plants, a visible senescence phenotype was observed only after week 7 in the long-day condition. Once senescence initiated, the progression of symptoms in the *atg* mutants was

faster than that in the wild type. Similar results were observed under short-day conditions, although the onset of visible senescence was later than under long-day conditions. The visible senescence phenotype was observed at around weeks 6 and 8 in *atg2* and *atg5*, respectively. At these stages, wild-type plants were still green and healthy. In both long- and short-day conditions, *atg2* exhibited a more severe phenotype than *atg5* for unknown reasons. In addition to the senescence phenotype, the *atg2* and *atg5* mutants showed growth retardation (Figures 1A and 3B). These results suggest that autophagy has an additional function apart from the role in recycling of proteins to serve as a source of amino acids in plants.

SA Is Hyperaccumulated in Autophagy-Defective Mutants

To investigate the novel role of plant autophagy under nutrient-rich conditions, we conducted phytohormone analyses in the wild type and *atg5*. Four-week-old plants grown on nutrient-rich soil under short-day conditions were used to minimize a potentially confounding influence of aging. Endogenous levels of SA, jasmonic acid (JA), jasmonic acid isoleucine (JA-Ile), gibberellin (GA$_1$ and GA$_4$), auxin (indole-3-acetic acid [IAA]), abscisic acid (ABA), cytokinin, and cytokinin derivatives (*trans*-zeatin [tZ], dihydrozeatin [DHZ], isopentenyladenine [iP], *trans*-zeatin riboside [tZR], and isopentenyl adenosine [iPR]) were measured using liquid chromatography-electrospray ionization tandem mass spectrometry (LC-ESI-MS/MS) (Table 1). We found that endogenous levels of SA were approximately threefold higher in *atg5* than in the wild type. The increase of SA levels was much more apparent in older (7-week-old) plants rather than younger (4-week-old) ones (see Supplemental Figure 1 online). Moreover, levels of JA and JA-Ile were increased approximately twofold in *atg5* mutants (Table 1). By contrast, IAA, ABA, and iP levels were only slightly increased in *atg5* when compared with the wild type. No significant difference was observed for the other phytohormones in wild-type and *atg5* plants.

To investigate the early senescence phenotype in the *atg* mutants at the transcriptional level, expression analyses were performed, especially focusing on senescence- and defense-related genes (Figure 2). We found that a senescence marker gene *SAG12* was not at detectable levels in the 3-week-old wild-type and *atg2* and *atg5* mutants, whereas *SAG12* transcripts accumulated to much higher levels in 4-week-old *atg2* and to a lesser extent in *atg5* than the wild type. The timing of these alterations in transcript levels correlates with the onset of visible senescence phenotype in the long- or short-day conditions. Transcript levels of the SA-responsive defense markers, *PR1* and *PR2*, were abundant in 3-week-old *atg2* and *atg5*, whereas transcript levels of these genes in the wild type remained low at this stage, consistent with the observation that SA hyperaccumulated in the *atg2* and *atg5* mutants. Transcript accumulation of *PDF1.2*, a JA-responsive marker, was also higher in the *atg2* and *atg5* mutants at this stage, whereas the transcript levels of *VSP2*, another JA-responsive marker, and *PAL*, another defense-related marker, were similar in the wild type and the *atg2* and *atg5* mutants. Taken together, these data suggest that SA signaling is activated in the *atg2* and *atg5* mutants before the onset of a visible senescence phenotype.
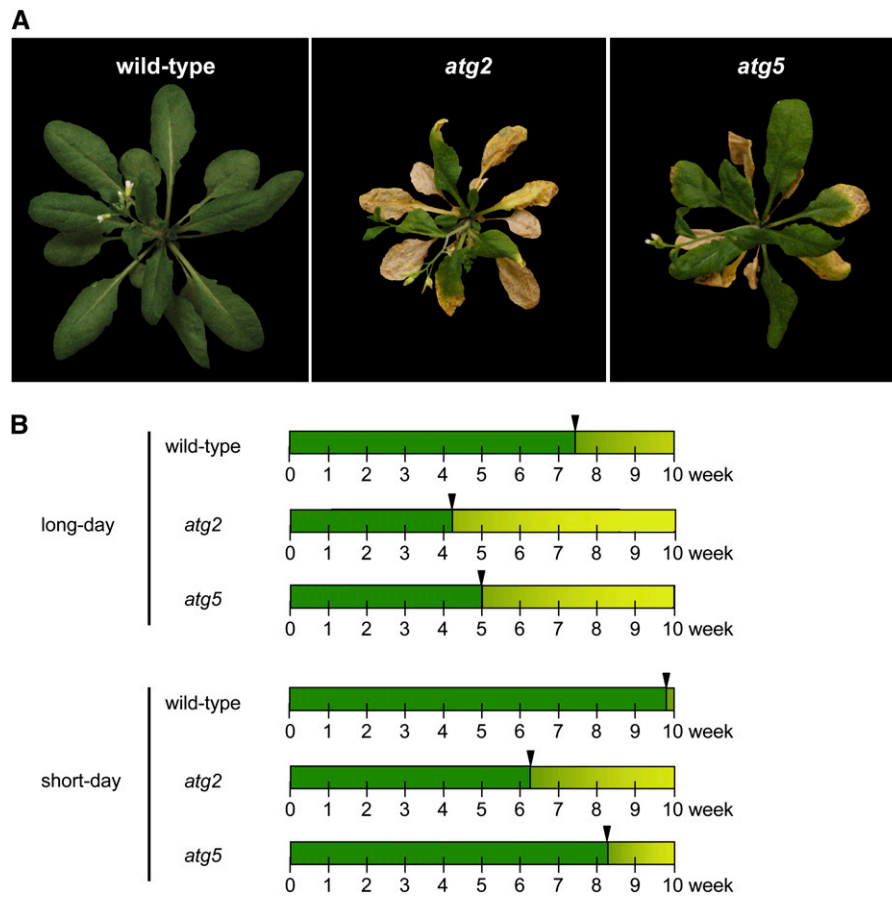
Figure 1. Early Senescence Phenotype of Autophagy-Defective Mutants under Nutrient-Rich Conditions.

(A) The wild type, *atg2*, and *atg5* mutant *Arabidopsis* were grown on vermiculite at 22°C with 16-h-light/8-h-dark cycles supplied with standard nutrient solution for 6 weeks.

(B) Schematic diagrams showing the onset of visible senescence in wild-type, *atg2*, and *atg5* mutant plants grown under long-day (16 h light/8 h dark) and short-day (8 h light/16 h dark) conditions. Senescence on the first and second leaves started around the time point shown by the arrowheads in our experimental conditions. Results were reproduced in at least five independent experiments using four or more plants in each experiment.

The Senescence Phenotype in *atg2* and *atg5* Mutants Is SA Dependent but JA and Ethylene Independent

To investigate if the early senescence phenotype in the *atg* mutants is SA dependent, we generated *atg2* and *atg5* mutants expressing the heterologous *NahG* transgene. Plants overexpressing *NahG* (*NahG* plants) completely suppressed the early senescence phenotype in both *atg2* and *atg5* (Figure 3A; see Supplemental Figure 2A online). To further confirm the SA dependence of the senescence phenotype, the *atg2* and *atg5* mutants were crossed to two other SA-related mutants, *sid2* and *npr1*. *SID2* encodes an isochorismate synthase, a rate-limiting enzyme for SA biosynthesis (Wildermuth et al., 2001), whereas *NPR1* encodes an ankyrin repeat protein that acts downstream of SA and regulates *PR1* expression through a direct interaction with a TGA-type bZIP transcription factor (Dong, 2004). Similar to *NahG* plants, both *sid2* and *npr1* suppressed the early senescence phenotype in *atg2* and *atg5* (Figure 3B; see Supplemental

Figure 2B online), although to a lesser extent in *sid2*, possibly due to the existence of other SA biosynthesis pathways.

Since JA and ethylene have been shown to modulate senescence pathways (Oh et al., 1997; He et al., 2002) and because *PDF1.2*, a JA marker, was induced in the *atg* mutants, we examined if the JA and ethylene pathways are also involved in the senescence phenotype in the *atg* mutants. For this purpose, we created *atg5 coi1*, *atg5 jar1*, and *atg5 ein2* double mutants. COI1 is an F-box protein that has a pivotal role in JA signaling, whereas JAR1 catalyzes the conjugation of JA to amino acids. Biological functions of EIN2 are still unclear, but it is required for general ethylene signaling. In contrast with *atg5 sid2*, *atg5 npr1*, and *NahG atg5* plants, these double mutants retained the early senescence phenotype in *atg5* even though JA and ethylene signaling were impaired (Figure 3B). Similar results were also obtained for the *atg2*-based double mutants, further supporting our hypothesis that JA and ethylene signaling are not required for

Table 1. Comprehensive Analysis of Phytohormones in Wild-Type and *atg5* Mutant Plants

Hormones (ng/gFW)	Wild Type	*atg5*
SA	53.3 ± 3.85	159.6 ± 32.2
JA	68.2 ± 28.1	141.9 ± 40.6
JA-Ile	5.50 ± 2.32	10.3 ± 4.13
GA$_1$	nd	nd
GA$_4$	0.11 ± 0.05	0.17 ± 0.09
IAA	5.00 ± 0.04	6.25 ± 0.25
ABA	5.28 ± 0.22	7.00 ± 0.21
tZ	0.43 ± 0.05	0.30 ± 0.01
DHZ	nd	nd
iP	0.05 ± 0.002	0.08 ± 0.001
tZR	1.44 ± 0.27	1.12 ± 0.15
iPR	0.75 ± 0.11	0.94 ± 0.13

Data represent the mean ± SD of three experiments. nd, not detected; FW, fresh weight.

the senescence phenotype in the *atg2* and *atg5* mutants (see Supplemental Figure 2B online).

Pathogen-Induced Spread of Chlorotic Cell Death in *atg5* Requires *SID2* and *NPR1*

Since autophagy deficiency leads to the spread of immunity-related PCD (Liu et al., 2005; Patel and Dinesh-Kumar, 2008), we investigated if this is also due to activation of the SA pathway. Infiltration of the avirulent bacterium *P. syringae* pv *tomato* bacteria DC3000 expressing *avrRpm1* (*Pst-avrRpm1*) into *atg5* leaves led to the spread of chlorotic cell death, whereas in the wild type, cell death was limited within the infected site (Figure 3C; see Supplemental Figure 3 online), consistent with previous reports. This phenotype was clearly seen in the older leaves of 7- to 8-week-old plants grown in the short-day condition; however, we noticed that in the younger leaves or at an early stage (4 to 5 weeks), no clear difference was detected between wild-type and *atg5* plants (data not shown). Thus, the phenotype is leaf age and plant age dependent. The growth of *Pst-avrRpm1* bacteria was not significantly different between wild-type and *atg5* plants, and the bacteria were not found in tissues outside the infection site (see Supplemental Figure 4 online). We also found that infiltration of *Pst-avrRpm1* did not lead to the spread of chlorotic cell death in the *atg5 sid2* and *atg5 npr1* double mutants (Figure 3C; see Supplemental Figure 3 online). Therefore, we concluded that the pathogen-induced spread of chlorotic cell death in autophagy-deficient plants requires the activation of the SA signaling pathway.

Dark-Induced Senescence and Growth Inhibition of Primary Roots under Nitrogen-Depleted Conditions Are Not Suppressed by Inactivation of SA Signaling

Previous reports have shown that autophagy-defective mutants exhibited a dark-induced senescence phenotype and reduced growth rate of primary roots under nutrient-starved conditions (Doelling et al., 2002; Hanaoka et al., 2002; Surpin et al., 2003; Yoshimoto et al., 2004; Thompson et al., 2005; Xiong et al., 2005; Patel and Dinesh-Kumar, 2008; Phillips et al., 2008). Consistent

with these reports, the *atg2* and *atg5* mutants induced senescence earlier than the wild type when 1-week-old seedlings were kept in the dark for 1 week. (Figure 4A, top and middle panels). In addition, detached leaves from 2-week-old *atg5* kept in the dark for several days exhibited senescence, whereas those of the wild type still remained green (Figure 4D). In contrast with the early senescence phenotype, these phenotypes were not suppressed by overexpression of the *NahG* gene (Figures 4A and 4D, bottom panels). Furthermore, when seedlings were grown on nitrogen-depleted medium for 14 d, the growth rate of primary roots in *atg5* was approximately half that of wild-type primary roots (Figures 4B and 4C). This phenotype was also not suppressed by overexpression of the *NahG* gene (Figures 4B and 4C). These results indicate that there are at least two different types of senescence phenotypes in the autophagy-defective mutants; one is an SA-dependent, developmentally controlled, early senescence phenotype and the other is an SA-independent, starvation- and dark-inducible phenotype.

BTH Sensitivity in the Autophagy-Defective Mutants Is NPR1 Dependent

To further characterize the SA-dependent senescence pathway in the *atg* mutants, the SA agonist BTH, which is not
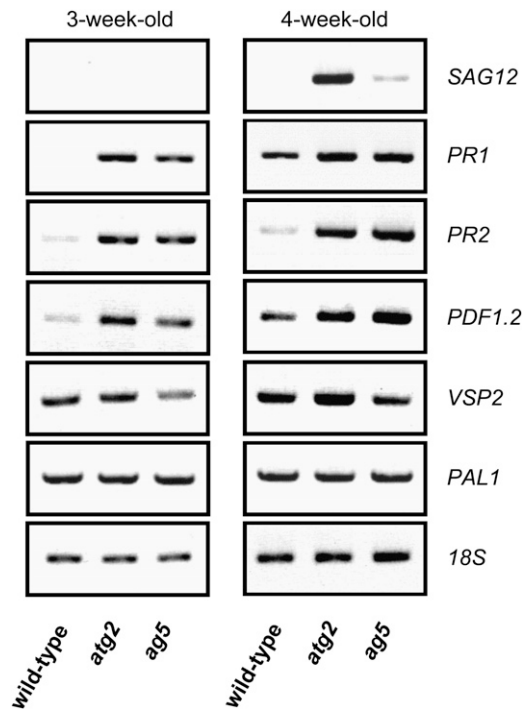

Figure 2. Expression Patterns of Senescence- or Pathogen-Related Genes in Wild-Type and Autophagy-Defective Mutant Plants.

Total RNAs from leaves of wild-type, *atg2*, and *atg5* plants grown on rockwool supplied with a rich nutrient solution for 3 to 4 weeks under long-day conditions were isolated and subjected to cycle-optimized RT-PCR using gene-specific primers and 18S rRNA as an internal control. SYBR-green was used for staining the gels. Gel pictures were rearranged for presentation purposes. Results were reproduced in three independent experiments.
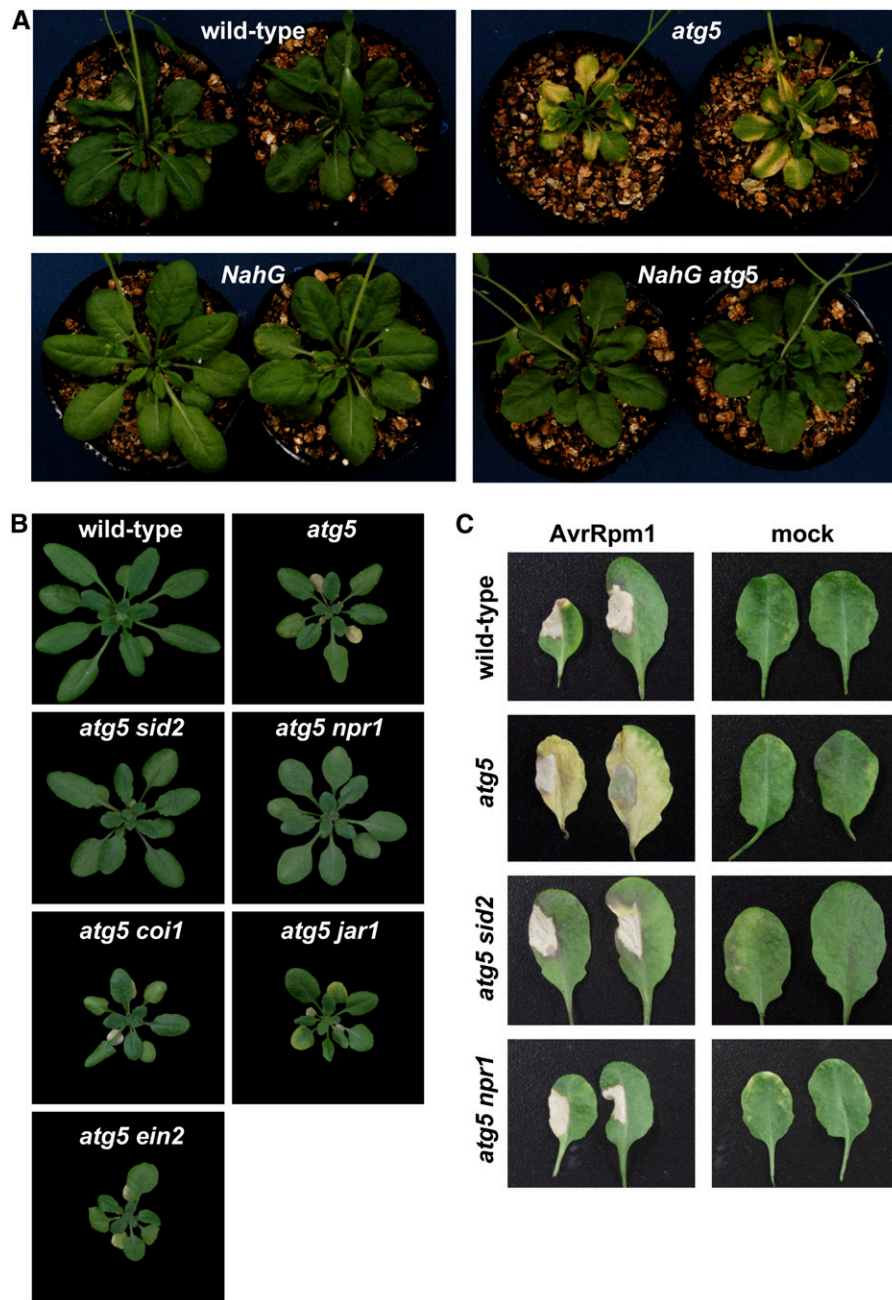
Figure 3. Early Senescence and Excessive Immunity-Related PCD Phenotypes of Autophagy-Defective Mutants Suppressed by Inactivation of the SA Signaling Pathway.

(A) The *NahG* gene was introduced into *atg5* by crossing. Photographs of 6-week-old plants of the indicated genotypes grown on vermiculite supplied with a rich nutrient solution under long-day conditions.

(B) The phenotype of the *atg5* double mutants with *sid2*, *npr1*, *coi1*, *jar1*, and *ein1*. Photographs of 5-week-old plants grown on rockwool supplied with a rich nutrient solution under long-day conditions.

(C) The fifth to eighth leaves of each plant grown under short-day conditions for 8 weeks were infected with *Pst-avrRpm1* (2×10^7 colony-forming units/mL) or 10 mM $MgCl_2$ (mock). Photographs were taken 9 d after infection. Results were reproduced in at least three independent experiments using four or more plants in each experiment.
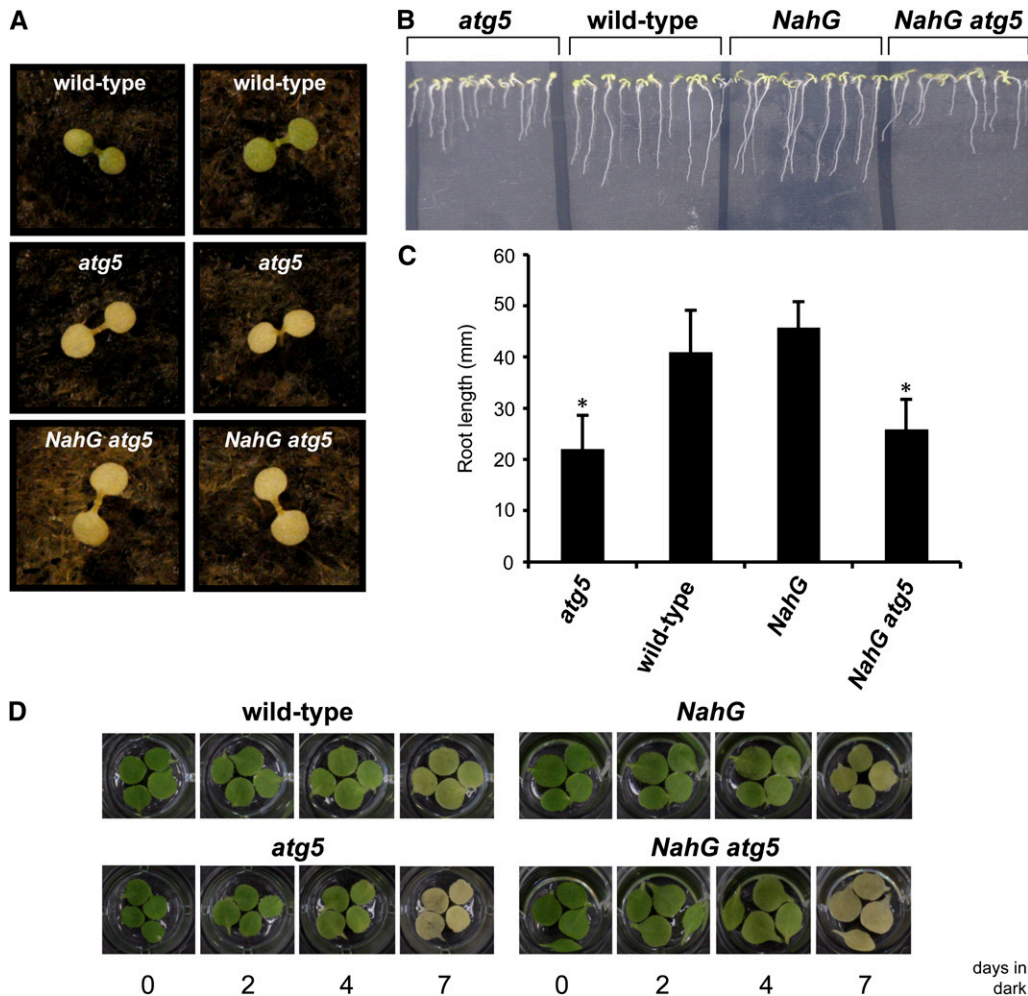
A

B   atg5   wild-type   NahG   NahG atg5

C

D   wild-type   NahG

atg5   NahG atg5

0   2   4   7   0   2   4   7   days in dark

Figure 4. The *atg*-Dependent Phenotypes That Are Not Suppressed by Inactivation of the SA Signaling Pathway.

(A) Dark-induced early senescence phenotype of *atg5* mutants is not suppressed by overexpression of the *NahG* gene. Seedlings of wild-type, *atg5*, and *NahG atg5* were grown under long-day conditions for 1 week, after which they were maintained in the dark. The photographs were taken 1 week after the beginning of the dark treatment.

(B) Reduced growth rate of the primary root of *atg* mutants under nitrogen-depleted conditions is not suppressed by *NahG*.

(C) Statistical evaluation of primary root length. Seeds of wild-type, *atg5*, *NahG*, and *NahG atg5* plants were sown on a nitrogen-free medium and, after 14 d, primary root length was measured using ImageJ. Error bars represent SD. All measurements were made on at least 10 individual plants. Asterisks indicate a significant difference from the wild type (P < 0.01; Student's *t* test).

(D) Phenotypes during artificially induced senescence. The first to fourth leaves of 2-week-old plants were detached and floated on 3 mM MES buffer, pH 5.7, at 22°C in the dark. The leaves were photographed at 0 d and after 2, 4, and 7 d of incubation. Representative leaves are shown.

catalyzed by *NahG*, was applied to *NahG atg5* plants and to *NahG* and wild-type plants as controls. As shown in Figure 5A, application of BTH to the *NahG atg5* plants restored senescence within a week, whereas wild-type and *NahG* plants were unaffected by this treatment. These results indicate that a BTH-inducible component(s) in the SA signaling pathway is required for the early senescence phenotype in the *atg* mutants. Since overexpression of *NahG* has a side effect due to accumulation of catechol, which is a by-product of SA degradation (Saskia and van Wees, 2003; van Wees and Glazebrook, 2003), *atg5*

sid2 plants were also treated with BTH to verify the above results. After BTH treatment, *atg5 sid2* plants exhibited a senescence phenotype, whereas no effects were observed in *sid2* (Figure 5B). Because most of the BTH-inducible genes are controlled by NPR1 (Wang et al., 2006), we investigated if the BTH effect on *atg5* is suppressed by *npr1*. Unlike *NahG atg5* and *atg5 sid2* plants, *atg5 npr1* double mutants did not show the early senescence phenotype after BTH treatments (Figure 5C). Thus, BTH hypersensitivity in the autophagy-defective mutants requires NPR1.
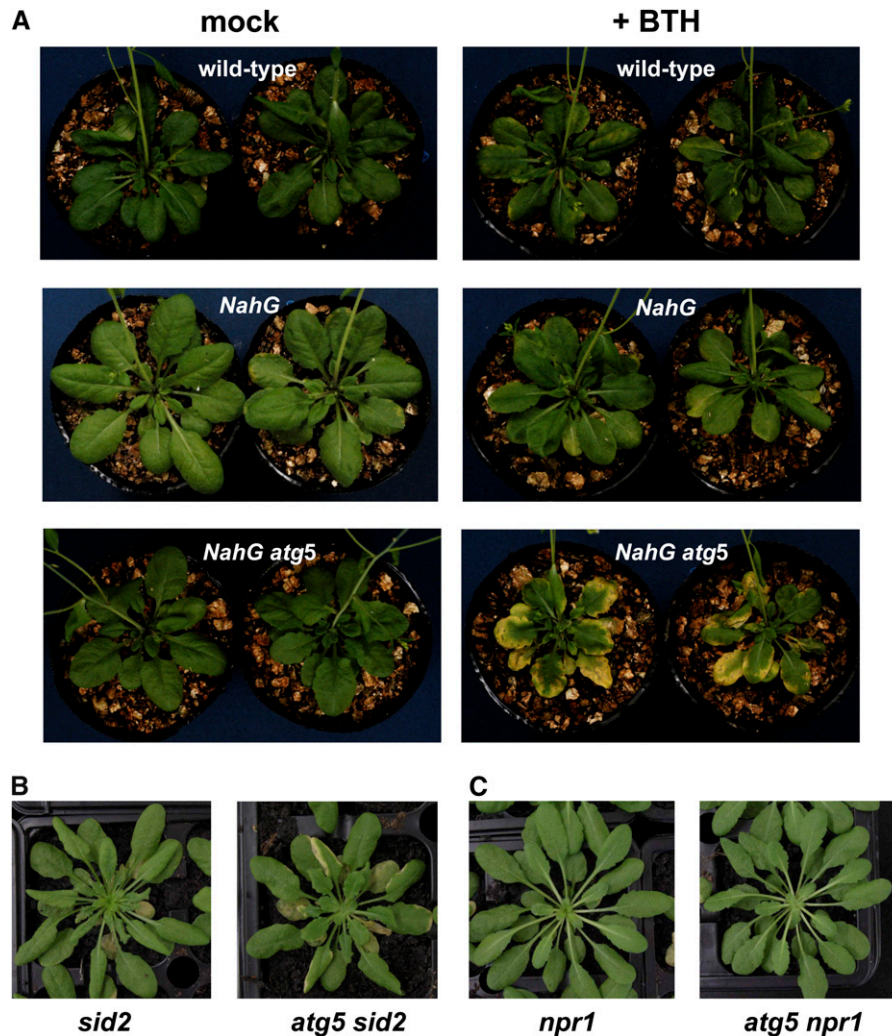
Figure 5. Phenotypes of BTH-Treated Wild-Type, *NahG*, *NahG atg5*, *sid2*, *atg5 sid2*, *npr1*, and *atg5 npr1* Plants.

(A) Mock-treated (left) and BTH-treated (right) wild-type, *NahG*, and *NahG atg5* plants 7 d after treatment. BTH (100 μM) was sprayed on 6-week-old plants grown under long-day conditions, and after 4 d it was repeated. Photographs were taken 3 d after the second BTH treatment.

(B) and **(C)** BTH-treated *sid2*, *atg5 sid2*, *npr1*, and *atg5 npr1* plants 10 d after treatment. BTH (100 μM) was sprayed on 7-week-old plants grown under short-day conditions, and after 4 d it was repeated. Then, after 6 d, photographs were taken. Results were reproduced in at least three independent experiments using four or more plants in each experiment.

Autophagy-Defective Mutants Accumulate High Levels of Reactive Oxygen Species

Leaf senescence is a form of PCD that is often associated with pronounced accumulation of reactive oxygen species (ROS) (Overmyer et al., 2003). Thus, we monitored levels of hydrogen peroxide (H_2O_2) in *atg2* and *atg5*, the SA-related mutants, and their double mutant combinations. Sixth or seventh leaves from 8-week-old plants grown under short-day conditions were stained with 3,3′-diaminobenzidine tetrahydrochloride (DAB), a histochemical reagent for H_2O_2 (Thordal-Christensen et al., 1997). Although these leaves showed no visible phenotypes (Figure 6, bottom panels), *atg2* and *atg5* leaves accumulated high levels of H_2O_2, whereas those of wild-type, *NahG*, *sid2*, and *npr1* showed much weaker staining, except for the vascular tissue (Figure 6, top and middle panels). Interestingly, *NahG atg5* and *atg5 sid2* plants, in which the early senescence phenotype in the *atg* mutant was suppressed, still exhibited enhanced accumulation of H_2O_2, although H_2O_2 levels appeared to be lower than those of *atg2* or *atg5* single mutants. In addition, *npr1 atg5* plants also showed enhanced accumulation of H_2O_2 compared with *npr1* plants (Figure 6, top panels). This accumulation of H_2O_2 in the *npr1 atg5* was also lower than those of *atg* single mutants. In summary, ROS accumulated in the *atg2* and *atg5* mutants in a partly SA-independent manner. These results suggest a partial role for autophagy in limiting ROS levels.
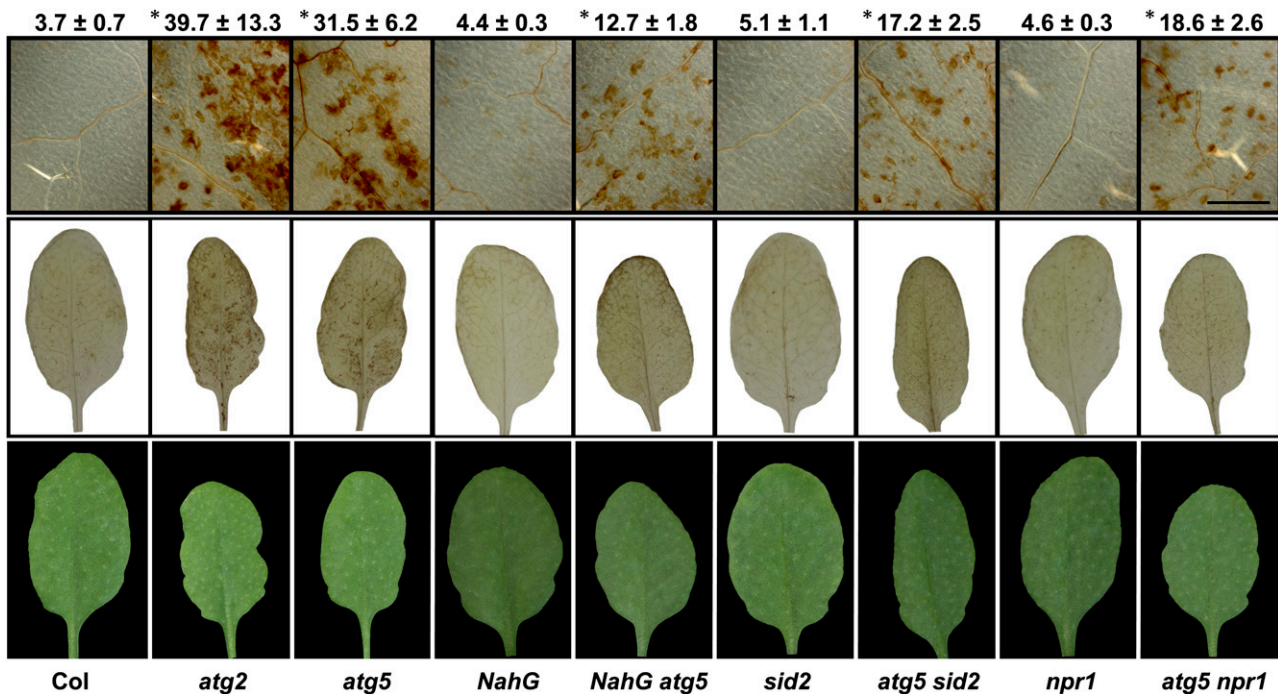
3.7 ± 0.7	*39.7 ± 13.3	*31.5 ± 6.2	4.4 ± 0.3	*12.7 ± 1.8	5.1 ± 1.1	*17.2 ± 2.5	4.6 ± 0.3	*18.6 ± 2.6

| Col | atg2 | atg5 | NahG | NahG atg5 | sid2 | atg5 sid2 | npr1 | atg5 npr1 |

Figure 6. DAB Staining of 8-Week-Old Plants Showing Sporadic Accumulation of Hydrogen Peroxide in Control Plants, *atg2* and *atg5* Mutants, and Lines Derived from Crosses with Mutants Defective in the SA Signaling Pathway.

Sixth or seventh leaves from 8-week-old plants grown under short-day conditions were detached and used for DAB staining. Representative leaves are shown. Numbers represent quantification of DAB staining as intensity per area from five leaves per genotype measured using ImageJ in arbitrary units with the mean ± 2 SD. Results were reproduced in three independent experiments using three plants in each experiment. Asterisks indicate a significant difference from the wild type (P < 0.01; Student's *t* test).

Autophagy Is Induced by SA Agonist Treatment

Since plant autophagy appears to be involved in the negative regulation of SA signaling, we examined the effect of BTH in induction of autophagosome formation in wild-type plants. For this purpose, we used green fluorescent protein (GFP)-tagged ATG8a as a marker for autophagy (Yoshimoto et al., 2004; Contento et al., 2005; Thompson et al., 2005). Roots of 7-d-old seedlings expressing GFP-ATG8a grown on nutrient-rich Murashige and Skoog (MS) solid medium were transferred to MS liquid medium with or without 100 μM BTH for 8 h and then observed by fluorescence microscopy. Numerous green dots or ring structures, likely representing pre-autophagosome or autophagosome structures, were detected in root cells after the BTH treatment, and less of these structures were present in nontreated root cells (Figures 7A and 7B). The results were further confirmed by the following cytological method. When roots of wild-type seedlings were treated with BTH and E-64d, a Cys protease inhibitor that blocks degradation in vacuole, autophagic bodies accumulated more rapidly compared with roots treated with E-64d alone (see Supplemental Figure 5 online). As expected, accumulation of autophagic bodies was not found in BTH-treated *atg2* and *atg5* mutant roots (see Supplemental Figure 5 online). The induction of autophagy by the SA agonist appears to be NPR1 dependent because *npr1* mutant roots did not show rapid accumulation of autophagic bodies after BTH

treatment (see Supplemental Figure 5 online). These observations imply that autophagy can be induced by SA and suggest that plant autophagy positively acts to eliminate SA signaling (Figure 7C).

DISCUSSION

The autophagy-defective *atg2* and *atg5* *Arabidopsis* mutants exhibited both an early senescence and an excessive immunity-related PCD regardless of nutrient conditions, suggesting that plant autophagy has an important regulatory role in a prosurvival function during such cell death progressions. Here, using biochemical, pharmacological, and genetic approaches, we have clearly demonstrated that excessive SA signaling is a major factor in *atg*-dependent chlorotic cell death.

Autophagy under Nutrient-Rich Conditions

Since autophagy is induced under starvation conditions, its physiological role had been thought to be nutrient recycling in general. Indeed, intracellular free amino acid levels decrease in autophagy-defective yeast cells (Onodera and Ohsumi, 2005) and mice (Kuma et al., 2004) under nutrient-limiting conditions; however, recent studies in mammals have indicated that autophagy plays much broader roles in many biological processes,
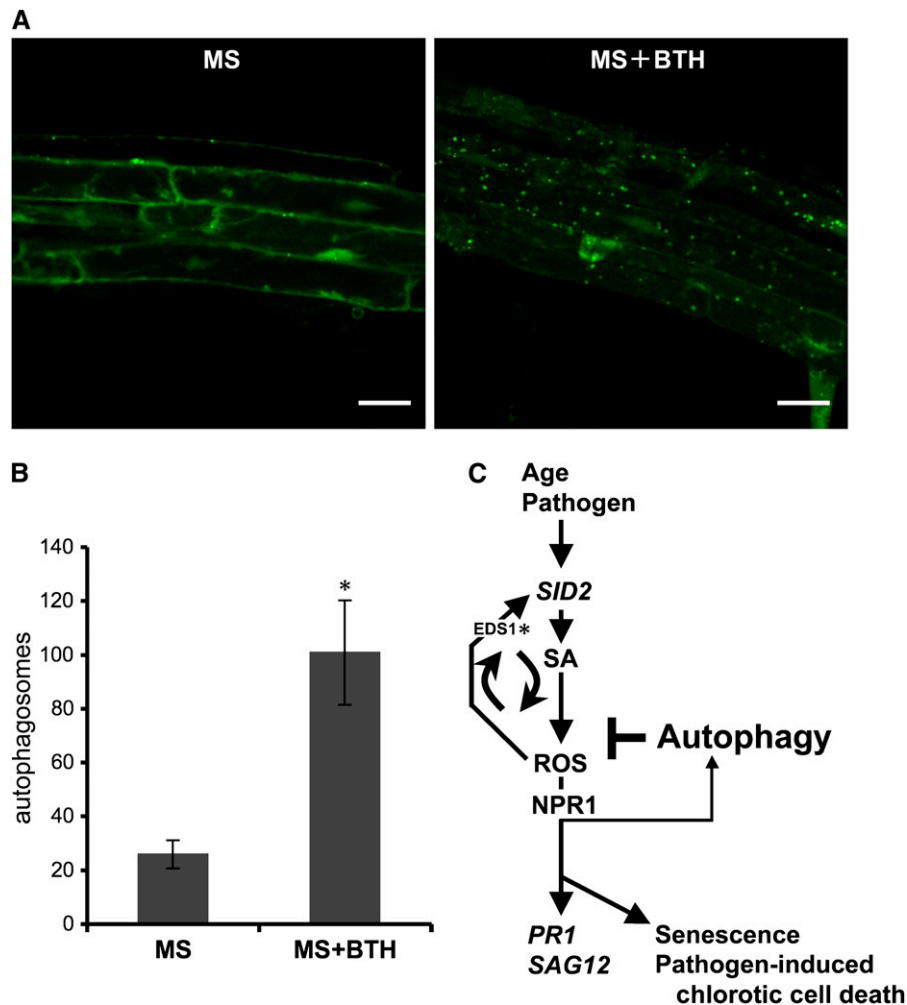
Figure 7. Negative Regulation of SA Signaling by Plant Autophagy.

(A) Autophagy is induced by BTH treatment. Roots of 7-d-old seedlings stably expressing GFP-ATG8a were excised and transferred to MS liquid medium with (right) or without (left) BTH (100 μM) for 8 h and then observed by fluorescence microscopy. Bars = 20 μm.

(B) Quantification of autophagosome-related structures. Numbers of autophagosome-related structures per root section were counted and the average number was determined for seven seedlings per treatment. Error bars indicate the SD. Results were reproduced in three independent experiments. An asterisk indicates a significant difference (P < 0.01; Student's *t* test).

(C) Hypothetical model for the role of autophagy during aging and immunity-related PCD. From this study, the following hypothetical model is proposed. During senescence and pathogen infection, SA signaling is accelerated by induction of SA biosynthesis, making an amplification loop through EDS1. Autophagy is induced by this SA signaling via NPR1 to operate a negative feedback loop modulating SA signaling that limits senescence and pathogen-induced chlorotic cell death. Based on Hofius et al. (2009) (*).

such as development, anti-aging, elimination of microorganisms, cell death, tumor suppression, and antigen presentation (Mizushima, 2005). In this study, we present several lines of evidence that plant autophagy has a role distinct from nutrient recycling. We found that the *atg2* and *atg5* mutants exhibit an early senescence phenotype under both short-day and long-day conditions even when nutrients are sufficient (Figure 1). Furthermore, our biochemical and molecular dissection revealed that the *atg5* mutants accumulate SA to high levels (Table 1) and express a senescence marker gene, *SAG12*, and SA-responsive defense marker genes, *PR1* and *PR2* (Figure 2), before showing

any microscopically visible phenotypes. Because there was no significant decrease in free amino acid levels in *atg5* compared with those in the wild type (see Supplemental Table 1 online), starvation is not likely to be the cause of such phenotypes. In addition, even under nutrient-rich conditions, ATG proteins are expressed throughout all developmental stages (Doelling et al., 2002; Hanaoka et al., 2002; Yoshimoto et al., 2004; Thompson et al., 2005; Phillips et al., 2008; Chung et al., 2009). These results strongly support the notion that plant autophagy has additional functions other than just recycling proteins as a source of amino acids.

Autophagy Negatively Regulates Cell Death via the SA Signaling Pathway during Aging and the Innate Immune Response

Our findings demonstrated that autophagy negatively regulates SA signaling, which is required for the early senescence phenotype, as well as for the excessive immunity-related PCD phenotype in the *atg* mutants. The importance of SA in senescence has been demonstrated by a report that transcript levels of *SAG12* and *PR1* were reduced in *NahG* plants, *pad4*, or *npr1*, and these SA-related mutant plants showed a delayed senescence phenotype (Morris et al., 2000); however, SA or BTH treatment alone was insufficient to induce senescence or immunity-related PCD in wild-type, *sid2*, or *NahG* plants (Figure 5). By contrast, BTH was able to induce the *atg*-dependent early senescence phenotype that was suppressed in the *NahG* or *sid2* background (Figure 5). Thus, apart from SA, there must be other factors regulating early senescence in the *atg2* and *atg5* mutants. These factors should function with NPR1 or its downstream component (s) because BTH is not able to override the *npr1*-dependent suppression of the early senescence in *atg5*.

A possible candidate for such factors is ROS since we found that autophagy also negatively regulates ROS accumulation. In yeast and mammals, cells lacking autophagy accumulate dysfunctional mitochondria, resulting in an increase in ROS production (Zhang et al., 2007; Tal et al., 2009). In *Arabidopsis*, however, high levels of H_2O_2 in the *atg2* and *atg5* mutants might not be due to dysfunctional mitochondria. Instead, high ROS accumulation in the *atg2* and *atg5* mutants was reduced to nearly one-half in the *NahG* and *sid2* background plants (Figure 6). Thus, ROS accumulated by both SA-dependent and SA-independent mechanisms in *atg2* and *atg5* mutant plants. Since increasing ROS levels induce SA biosynthesis (Neuenschwander et al., 1995, Takahashi et al., 1997, Chamnongpol et al., 1998), SA and ROS are likely to form a positive amplification loop (Shah, 2003; Figure 7). The cellular redox state modulated by SA-ROS amplification can be sensed by NPR1 (Mou et al., 2003). This observation may explain why chlorotic cell death in the *atg2* and *atg5* mutants is suppressed by *npr1*, and even exogenous application of BTH is not able to recover the phenotype.

What could be the physiological role(s) of autophagy during cell death in plants? The fact that SA signaling is activated in the *atg2* and *atg5* mutants led us to hypothesize that autophagy is induced to eliminate SA signaling during aging and immunity-related PCD. Using an autophagosome marker, GFP-ATG8a, a number of autophagosomes were detected in wild-type root cells after 8 h of BTH treatment, but significantly fewer autophagosomes were observed in nontreated cells (Figures 7A and 7B), implying that autophagy is induced by SA. This result is consistent with an earlier report that autophagy is induced by pathogen infections (Liu et al., 2005). In addition, although the molecular mechanism is still unclear, autophagy can be induced by H_2O_2 in *Arabidopsis* (Xiong et al., 2007). In mammalian cells, autophagy also can be induced by H_2O_2 via ATG4 protein activity (Scherz-Shouval et al., 2007). These findings suggest a hypothetical model in which autophagy actively downregulates SA-ROS amplification signaling that controls cell death during aging and immunity-related PCD (Figure 7C).

Autophagy-Defective Mutants Are Similar to *mlo2*, a Powdery Mildew–Resistant Mutant, with Regard to the Age-Related Early Cell Death Phenotype

While carrying out the phenotypic analyses, we noticed similarities in the phenotypes between *atg2* and *atg5* and the *mlo2* mutants in *Arabidopsis*. *Arabidopsis mlo2* exhibits resistance to a virulent powdery mildew pathogen, *Golovinomyces orontii* (Consonni et al., 2006). In addition to resistance to powdery mildew, *mlo2* also shows a developmentally controlled early senescence phenotype that is accompanied by the accumulation of H_2O_2. Reminiscent of *atg2* and *atg5* mutants, the *mlo2*-mediated early senescence phenotype is suppressed by inactivation of SA signaling but not by inactivation of JA or ethylene signaling. In addition, *mlo2* exhibits a developmentally controlled increase in SA levels that precedes the onset of the visible senescence phenotypes. Furthermore, we found that, similar to *atg2* and *atg5* mutants, BTH treatments restore the *mlo2*-dependent early senescence phenotype in the *NahG* or *sid2* background (see Supplemental Figure 6 online). Similarities between *atg5* and *mlo2* were further highlighted by the fact that the early senescence phenotype in both *atg5* and *mlo2* was accelerated by *pen1* and partially suppressed by *pen2* (see Supplemental Figure 7 online; Consonni et al., 2006); however, unlike *mlo2*, *atg2* and *atg5* mutants did not exhibit significant resistance to powdery mildew (see Supplemental Figure 8 online), indicating that these mutants are similar to *mlo2* only with regard to the early senescence phenotype. In fact, powdery mildew resistance in *mlo2* was not dependent on SA (Consonni et al., 2006). Similar to its barley (*Hordeum vulgare*) ortholog, MLO2 is thought to function as a modulator of SNARE protein-dependent and vesicle transport-associated processes at the plasma membrane (Panstruga, 2005). Consequently, loss of MLO2 may cause the accumulation of particular vesicle populations that result in the age-related early cell death phenotype. In this scenario, autophagy may be involved in degradation of such vesicles, and the normal level of autophagy may not be sufficient for removing an increased number of vesicles, thus leading to similar senescence phenotypes.

Does Autophagy Have a Pro-Death Function in Plants?

Morphological studies suggested that autophagic processes execute developmental PCD in plants (Matile and Winkenbach, 1971; Smith et al., 1992; Filonova et al., 2000). However, various *atg* mutants that completely lack autophagy could achieve normal embryogenesis, seed germination, xylem differentiation, root development, and petal senescence, processes that were previously assumed to involve autophagic cell death (Lam, 2004; Bozhkov et al., 2005; van Doorn and Woltering, 2005, 2008). Recently, Hofius et al. (2009) proposed that autophagy has a pro-death function during *Pst-avrRps4*–induced cell death in *Arabidopsis*, as partially reduced cell death rates, measured by an ion leakage assay, were detected in autophagy-defective mutants. The pro-death function appears to be very specific as only minor or no reduction of cell death was observed when *Pst-avrRpm1* or *Pst-avrRpt2* was used. Interestingly, however, both *Pst-avrRps4* and *Pst-avrRpm1* clearly induced cell death lesions at the

The Plant Cell

infection site, and no spread of chlorotic cell death was observed (Hofius et al., 2009). This is markedly different from what we and others observed (Figure 3C; Liu et al., 2005). This apparent discrepancy can be explained by our observation that the spreading cell death phenotype of the *atg2* and *atg5* mutants was only seen in older leaves of older plants, not in younger plants or younger leaves. The age dependency is likely due to the developmentally controlled increase of SA levels in the *atg2* and *atg5* mutants (see Supplemental Figure 1 online). It is possible that in case of *Pst-avrRps4*, proper SA levels are critical to fully execute cell death. Consistent with this possibility, EDS1, a modulator of SA amplification signal, is important for *Pst-avrRps4*–dependent SA induction (Feys et al., 2001) as well as for *Pst-avrRps4*–dependent autophagy induction (Hofius et al., 2009). These facts suggest that SA can induce autophagy, further supporting our model (Figure 7C).

In mammalian cells, autophagy can also be a part of the cell death mechanism (Levine and Yuan, 2005). The interaction between anti-apoptotic Bcl2 protein and ATG6/Beclin1 governs the threshold for transition from cell survival to cell death (Pattingre et al., 2005). In most of these cases, apoptosis-associated proteins, such as caspases, Bax, Bak, and Bcl2, were related to these autophagic cell death phenotypes; however, orthologs of these proteins have not been identified at the primary sequence level in plant genomes. Thus, unlike in mammals, plant autophagy may not have such a pro-death function. However, we cannot exclude the possibility that excessive autophagy promotes programmed cell death under some specific condition in plants, since plants might have functional homologs of apoptosis-related proteins. Further analyses using NahG *atg*, *atg sid2*, or *atg npr1* plants, in which the early senescence phenotype is suppressed, and further identification of functional homologs of apoptosis-related proteins would help to unravel the potential pro-death function in plant autophagy.

METHODS

Plant Material and Growth Conditions

Arabidopsis thaliana ecotype Columbia was used in this study. The seeds of T-DNA knockout mutants of ATG2 and ATG5 (*atg2-1* [SALK_076727] and *atg5-1* [SAIL_129B07], respectively) were obtained from the Nottingham Arabidopsis Resource Center. Homozygous plants were isolated by PCR as described by Inoue et al. (2006). For long-day conditions, plants were grown on rockwool or vermiculite at 22°C with 16-h-light/8-h-dark cycles using hydroponic media for nutrients. For short-day conditions, plants were grown on soil at 22°C with 8-h-light/16-h-dark cycles. For plate-grown plants, seeds were surface sterilized, chilled at 4°C for 4 d, and then sown and grown on MS or nitrogen-depleted MS medium (MS-N). The MS-N medium was prepared by depleting the NH_4NO_3 and replacing the KNO_3 with KCl.

Quantification of Phytohormones

Phytohormones were quantified using a 6410 Triple Quad LCMS (Agilent) that includes an Agilent 1200 series rapid resolution liquid chromatography system fitted with a ZORBAX Eclipse XDB-C18 column (1.8 μm, 2.1 × 50 mm). d_2-GA$_1$, d_2-GA$_4$, d_5-tZ, d_3-DHZ, d_6-iP, d_5-tZR, and d_6-iPR obtained from OlChemIm, d_6-ABA obtained from Icon Isotopes, d_2-IAA and d_6-SA obtained from Sigma-Aldrich, d_2-JA obtained from Tokyo

Kasei, and synthesized $^{13}C_6$-JA-Ile (Jikumaru et al., 2004) were used as internal standards. Aerial parts of *Arabidopsis* grown for 4 weeks were frozen with liquid nitrogen, ground with 10-mm ceramic beads, and extracted with 5 volumes of 80% (v/v) methanol containing 1% (v/v) acetic acid and internal standards for 1 h. Extracts were centrifuged at 4°C, 14,000*g*, 10 min, and the supernatant was collected. This procedure was repeated once, and methanol was removed in a SpeedVac (Thermo Fisher). Acidic water extracts were loaded onto an Oasis HLB extraction cartridge (30 mg, 1 mL; Waters) and washed with 1 mL of water containing 1% acetic acid to segregate high polar impurities. Phytohormones were eluted with 2 mL of 80% methanol containing 1% acetic acid, and the methanol in this eluent was removed in a SpeedVac. Acidic water extracts were loaded onto an Oasis MCX extraction cartridge (30 mg, 1 mL). After washing with 1 mL of water containing 1% acetic acid, acidic and neutral compounds were eluted with 2 mL of methanol (AN fraction). After washing with water containing 5% (v/v) ammonia, basic compounds were eluted with 2 mL of 60% (v/v) methanol containing 5% (v/v) ammonia. After drying these basic fractions, 20 μL of water containing 1% acetic acid was added and the basic hormones (tZ and iP) in these fractions were analyzed by LC-MS/MS. Subfractions (10%) of the AN fractions were collected and prepared as basic fractions to analyze for SA. The remaining 90% of the AN fractions were concentrated to acidic water in the SpeedVac to remove methanol and loaded onto Oasis WAX extraction cartridges (30 mg, 1 mL). After washing with 1 mL of water containing 1% acetic acid, neutral compounds were eluted with 2 mL of methanol, and acidic compounds were eluted with 2 mL of 80% methanol containing 1% acetic acid. After concentrating these acidic fractions to dryness, 20 μL of water containing 1% acetic acid was added and acidic hormones (IAA, ABA, JA, JA-Ile, GA$_1$, and GA$_4$) in these fractions were analyzed. LC conditions and parameters for LC-ESI-MS/MS analysis are described in Supplemental Tables 2 and 3 online.

Expression Analyses

To examine the expression of senescence- and defense-related genes, such as *SAG12*, *PR1*, *PR2*, *PDF1.2*, *VSP2*, and *PAL1*, total RNA was isolated from leaves using the RNeasy plant mini kit (Qiagen). The isolated total RNA was treated with DNase (Takara) prior to the synthesis of first-strand cDNA by the SuperScript III first-strand synthesis system with oligo(dT)$_{20}$ primer (Invitrogen). cDNA derived from 0.2 μg of total RNA was used as a template for each PCR reaction. Gene-specific primers used are as follows: for *SAG12*, 5′-CTTTGTCAGAACAGCTTG-3′ and 5′-ATGGCAAGACCACATAGTCC-3′; for *PR1*, 5′- CGTCTTTGTAGC-TCTTGTAGGTGCTCTTGTTC-3′ and 5′-GTATGGCTTCTCGTTCACATA-ATTCCCACGAG-3′; for *PR2*, 5′-ATGTCTGAATCAAGGAGCTTAGCCT-CACCACC-3′ and 5′-GTTGAAATTAACTTCATACTTAGACTGTCGAT-CTGG-3′; for *PDF1.2a*, 5′-ATGGCTAAGTTTGCTTCCATCATCACCCT-TATC-3′ and 5′-CATGGGACGTAACAGATACACTTGTGTGCTGGG-3′; for *VSP2*, 5′-CTTTCACTTCTCTTGCTCTTGGCCGCTAC-3′ and 5′-GAG-TGGATTTGGGAGCTTAAAAACCCTCCC-3′; for *PAL1*, 5′-ATGGAGAT-TAACGGGGCACACAAGAGCAACGGAG-3′ and 5′-CAACAGCTTCA-GAAGTTTTGCGAGACGAGATTAG-3′ and QuantumRNA 18S internal standards for 18S rRNA (Ambion). PCR was terminated after 24 cycles for *SAG12*, *PR1*, *PR2*, *PDF1.2a*, *VSP2*, *PAL1*, and 20 cycles for 18S rRNA to ensure that the RT-PCR was in the logarithmic amplification range. The products were electrophoresed on a gel containing SYBR Green I (Takara) and detected using a CCD camera with SYBR Green fluorescence filter.

Genetic Analyses

Homozygous *NahG* in ecotype Col-0 (B15; Delaney et al., 1994), obtained from Syngenta Biotechnology, was crossed to *atg2* and *atg5*, respectively. The F3 seeds were sown on MS medium, and then *atg2* and *atg5*

mutants homozygously expressing the *NahG* gene were identified by PCR using gene-specific primers. Gene-specific primers used are as follows: for verifying *atg2* mutant, 5′-GCGTGGACCGCTTGCTGCAACT-3′ designated as LBb1, and 5′-GCTAGCATCTATTTGGTCAC-3′ and 5′-CATTCGAGGTTCTGGCCTAAC-3′; for *atg5* mutant, 5′-TAGCATC-TGAATTTCATAACCAATCTCGATACAC-3′ designated as LB3, and 5′-ATTCACTTCCTCCTGGTGAAG-3′ and 5′-TTGTGCCTGCAGGATA-AGCG-3′; for *NahG*, 5′-ATGAAAAACAATAAACTTGGCTTGCGCATCGG-TATCG-3′ and 5′-CGTCCTCAAGCCCTTGGCCAGCACCGGCAC-3′.

Arabidopsis mutant alleles *sid2-2* (Dewdney et al., 2000), *npr1-1* (Cao et al., 1997), *jar1-1* (Staswick et al., 2002), *coi1-1* (Xie et al., 1998), and *ein2-1* (Alonso et al., 1999) were used for intermutant crosses with either *atg2* or *atg5*. *atg sid2* was identified by PCR using the following gene-specific primers: 5′-TTCTTCATGCAGGGGAGGAG-3′ and 5′-CAACCA-CCTGGTGCACCAGC-3′ and 5′-AAGCAAAATGTTTGAGTCAGCA-3′. Only the 879-bp fragment was amplified from homozygous Col-0, two fragments (879 and 581 bp) were amplified from heterozygous plants, and only the 581-bp fragment was amplified from homozygous *sid2-2*. *atg npr1* was constructed by cleaved-amplified polymorphic sequence (CAPS) selection of *npr1-1* homozygous F3 families by use of the *Nla* III polymorphism of *npr1-1*. *atg jar1* was selected by CAPS using *Hpy188* III polymorphism. For isolation of *atg coi1*, first *atg/atg COI1/coi1* was selected by CAPS using *Xcm*I polymorphism as described before (Xie et al., 1998). Then, double mutants segregating from the *atg/atg COI1/coi1* were used for phenotypic analyses. *atg ein2* was constructed by selection of kanamycin-resistant F2 seedlings insensitive to 500 μM 1-aminocyclopropane-1-carboxylic acid. After the selection, sequencing of *EIN2* in *atg ein2* confirmed that the mutant was homozygous for the *ein2-1* allele.

Phenotypic Analyses

Phenotypic analyses were performed as described previously (Hanaoka et al., 2002; Yoshimoto et al., 2004), except for examination of pathogen infection. For observation of the pathogen-induced cell death phenotype, seeds were sown on soil and grown under short-day conditions for 8 weeks, and then *Pst-avrRpm1* (2×10^7 colony-forming units/mL) or 10 mM MgCl$_2$ (mock) was hand-infiltrated using a needleless syringe. After the infection, plants were transferred to continuous light conditions for 9 d and then photographs were taken.

BTH Treatment

BTH dissolved in water (100 μM) was sprayed on 6- or 7-week-old plants grown under long- or short-day conditions, respectively, and repeated after 4 d. Photographs were taken 3 or 6 d after the last treatment.

Cytology

To assay for H$_2$O$_2$ accumulation, leaves were stained with DAB. The sixth or seventh leaves from 8-week-old plants grown under short-day conditions were detached and quickly vacuum-infiltrated with the DAB solution. Then, the leaves were incubated in the dark for 8 h. Before observation by light microscopy, the leaves were destained with lactic acid/glycerol/ethanol (1:1:3) and cleared with chloral hydrate (5 mg/mL). DAB staining was quantified by intensity per area using ImageJ 1.38.

To visualize induction of autophagy by BTH, stable transformants constitutively expressing a GFP-ATG8a fusion protein (Yoshimoto et al., 2004) were generated in the Col-0 background. *Arabidopsis* transformation was conducted as described by Yoshimoto et al. (2004). Primary roots of transgenic plants expressing GFP-ATG8a grown on MS solid medium for 1 week were cut and transferred to MS liquid medium with or without BTH (100 μM) for 8 h and then observed with a Zeiss LSM510 META confocal laser scanning microscope using a 488/568-nm ArKr

laser in combination with a 505- to 550-nm band-pass filter set. Image acquisition and processing were performed using a Zeiss laser scanning microscope (LSM 510, version 3.2) and Adobe Photoshop Element 5.0 (Adobe Systems).

Accession Numbers

Sequence data from this article can be found in the Arabidopsis Genome Initiative or GenBank/EMBL databases under the following accession numbers: *ATG2* (At3g19190), *ATG5* (At5g17290), *SAG12* (At5g45890), *PR1* (At2g14610), *PR2* (At3g57260), *PDF1.2a* (At5g44420), *VSP2* (At5g24770), *PAL1* (At2g37040), *SID2* (At1g74710), *NPR1* (At1g64280), *JAR1* (At2g46370), *COI1* (At2g39940), *EIN2* (At5g03280), and *MLO2* (At1g11310).

Supplemental Data

The following materials are available in the online version of this article.

Supplemental Figures 1. The *atg5* Mutant Shows a Developmentally Controlled Increase in SA Levels.

Supplemental Figure 2. Early Senescence Phenotype of Autophagy-Defective Mutants Was Suppressed by Inactivation of the SA Signaling Pathway.

Supplemental Figure 3. Pathogen-Induced Chlorotic Cell Death Suppressed by SA Signaling Pathway.

Supplemental Figure 4. Bacterial Growth Analysis of *Pst-avrRpm1* in Wild-Type and *atg5* Plants.

Supplemental Figure 5. Autophagy Is Induced by BTH Treatment.

Supplemental Figure 6. Phenotypes of BTH-Treated *mlo2-5*, *mlo2-11*, *NahG mlo2-5*, *NahG mlo2-11*, and m*lo2-11 sid2* Plants.

Supplemental Figure 7. Early Senescence Phenotype of Autophagy-Defective Mutants Was Accelerated by *pen1* and Partially Suppressed by *pen2*.

Supplemental Figure 8. The *atg* Mutants Do Not Show Obvious Resistance against a Powdery Mildew, *G. orontii*, Unlike *mlo2*.

Supplemental Table 1. Relative Levels of Free Amino Acids on Wild-Type and *atg5* Mutant Plants.

Supplemental Table 2. LC Conditions.

Supplemental Table 3. Parameters for LC-ESI-MS/MS Analysis (Agilent 1200-6410).

Supplemental Methods.

Supplemental References.

REFERENCES

Alonso, **J.M.**, **Hirayama**, **T.**, **Roman**, **G.**, **Nourizadeh**, **S.**, **and Ecker**, **J.R.** (1999). EIN2, a bifunctional transducer of ethylene and stress responses in *Arabidopsis.* Science **284:** 2148–2152.

Barth, **H.**, **Meiling-Wesse**, **K.**, **Epple**, **U.D.**, **and Thumm**, **M.** (2001). Autophagy and the cytoplasm to vacuole targeting pathway both require Aut10p. FEBS Lett. **508:** 23–28.

Bassham, **D.C.**, **Laporte**, **M.**, **Marty**, **F.**, **Moriyasu**, **Y.**, **Ohsumi**, **Y.**, **Olsen**, **L.J.**, **and Yoshimoto**, **K.** (2006). Autophagy in development and stress responses of plants. Autophagy **2:** 2–11.

Bozhkov, **P.V.**, **Suarez**, **M.F.**, **Filonova**, **L.H.**, **Daniel**, **G.**, **Zamyatnin**, **A.A.**, **Jr.**, **Rodriguez-Nieto**, **S.**, **Zhivotovsky**, **B.**, **and Smertenko**, **A.** (2005). Cysteine protease mcII-Pa executes programmed cell death during plant embryogenesis. Proc. Natl. Acad. Sci. USA **102:** 14463–14468.

Cao, **H.**, **Glazebrook**, **J.**, **Clarke**, **J.D.**, **Volko**, **S.**, **and Dong**, **X.** (1997). The *Arabidopsis* NPR1 gene that controls systemic acquired resistance encodes a novel protein containing ankyrin repeats. Cell **88:** 57–63.

Chamnongpol, **S.**, **Willekens**, **H.**, **Moeder**, **W.**, **Langebartels**, **C.**, **Sandermann**, **H.**, **Jr.**, **Van Montagu**, **M.**, **Inzé**, **D.**, **and Van Camp**, **W.** (1998). Defense activation and enhanced pathogen tolerance induced by H_2O_2 in transgenic tobacco. Proc. Natl. Acad. Sci. USA **95:** 5818–5823.

Chung, **T.**, **Suttangkakul**, **A.**, **and Vierstra**, **R.D.** (2009). The ATG autophagic conjugation system in maize: ATG transcripts and abundance of the ATG8-lipid adduct are regulated by development and nutrient availability. Plant Physiol. **149:** 220–234.

Consonni, **C.**, **Humphry**, **M.E.**, **Hartmann**, **H.A.**, **Livaja**, **M.**, **Durner**, **J.**, **Westphal**, **L.**, **Vogel**, **J.**, **Lipka**, **V.**, **Kemmerling**, **B.**, **Schulze-Lefert**, **P.**, **Somerville**, **S.C.**, **and Panstruga**, **R.** (2006). Conserved requirement for a plant host cell protein in powdery mildew pathogenesis. Nat. Genet. **38:** 716–720.

Contento, **A.L.**, **Xiong**, **Y.**, **and Bassham**, **D.C.** (2005). Visualization of autophagy in *Arabidopsis* using the fluorescent dye monodansylcadaverine and a GFP-AtATG8e fusion protein. Plant J. **42:** 598–608.

Delaney, **T.P.**, **Uknes**, **S.**, **Vernooij**, **B.**, **Friedrich**, **L.**, **Weymann**, **K.**, **Negrotto**, **D.**, **Gaffney**, **T.**, **Gut-Rella**, **M.**, **Kessmann**, **H.**, **Ward**, **E.**, **and Ryals**, **J.** (1994). A central role of salicylic acid in plant disease resistance. Science **266:** 1247–1250.

Dewdney, **J.**, **Reuber**, **T.L.**, **Wildermuth**, **M.C.**, **Devoto**, **A.**, **Cui**, **J.**, **Stutius**, **L.M.**, **Drummond**, **E.P.**, **and Ausubel**, **F.M.** (2000). Three unique mutants of *Arabidopsis* identify *eds* loci required for limiting growth of a biotrophic fungal pathogen. Plant J. **24:** 205–218.

Doelling, **J.H.**, **Walker**, **J.M.**, **Friedman**, **E.M.**, **Thompson**, **A.R.**, **and Vierstra**, **R.D.** (2002). The APG8/12-activating enzyme APG7 is required for proper nutrient recycling and senescence in *Arabidopsis thaliana.* J. Biol. Chem. **277:** 33105–33114.

Dong, **X.** (2004). NPR1, all things considered. Curr. Opin. Plant Biol. **7:** 547–552.

Feys, **B.J.**, **Moisan**, **L.J.**, **Newman**, **M.A.**, **and Parker**, **J.E.** (2001). Direct interaction between the *Arabidopsis* disease resistance signaling proteins, EDS1 and PAD4. EMBO J. **20:** 5400–5411.

Filonova, **L.H.**, **Bozhkov**, **P.V.**, **Brukhin**, **V.B.**, **Daniel**, **G.**, **Zhivotovsky**, **B.**, **and von Arnold**, **S.** (2000). Two waves of programmed cell death occur during formation and development of somatic embryos in the gymnosperm, Norway spruce. J. Cell Sci. **113:** 4399–4411.

Hanaoka, **H.**, **Noda**, **T.**, **Shirano**, **Y.**, **Kato**, **T.**, **Hayashi**, **H.**, **Shibata**, **D.**, **Tabata**, **S.**, **and Ohsumi**, **Y.** (2002). Leaf senescence and starvation-induced chlorosis are accelerated by the disruption of an *Arabidopsis* autophagy gene. Plant Physiol. **129:** 1181–1193.

He, **Y.**, **Fukushige**, **H.**, **Hildebrand**, **D.F.**, **and Gan**, **S.** (2002). Evidence supporting a role of jasmonic acid in *Arabidopsis* leaf senescence. Plant Physiol. **128:** 876–884.

Hofius, **D.**, **Schultz-Larsen**, **T.**, **Joensen**, **J.**, **Tsitsigiannis**, **D.I.**, **Petersen**, **N.H.**, **Mattsson**, **O.**, **Jørgensen**, **L.B.**, **Jones**, **J.D.**, **Mundy**, **J.**, **and Petersen**, **M.** (2009). Autophagic components contribute to hypersensitive cell death in *Arabidopsis.* Cell **137:** 773–783.

Inoue, **Y.**, **Suzuki**, **T.**, **Hattori**, **M.**, **Yoshimoto**, **K.**, **Ohsumi**, **Y.**, **and Moriyasu**, **Y.** (2006). *AtATG* genes, homologs of yeast autophagy genes, are involved in constitutive autophagy in *Arabidopsis* root tip cells. Plant Cell Physiol. **47:** 1641–1652.

Ishida, **H.**, **Yoshimoto**, **K.**, **Izumi**, **M.**, **Reisen**, **D.**, **Yano**, **Y.**, **Makino**, **A.**, **Ohsumi**, **Y.**, **Hanson**, **M.R.**, **and Mae**, **T.** (2008). Mobilization of rubisco and stroma-localized fluorescent proteins of chloroplasts to the vacuole by an ATG gene-dependent autophagic process. Plant Physiol. **148:** 142–155.

Jikumaru, **Y.**, **Asami**, **T.**, **Seto**, **H.**, **Yoshida**, **S.**, **Yokoyama**, **T.**, **Obara**, **N.**, **Hasegawa**, **M.**, **Kodama**, **O.**, **Nishiyama**, **M.**, **Okada**, **K.**, **Nojiri**, **H.**, **and Yamane**, **H.** (2004). Preparation and biological activity of molecular probes to identify and analyze jasmonic acid-binding proteins. Biosci. Biotechnol. Biochem. **68:** 1461–1466.

Klionsky, **D.J.** (2005). The molecular machinery of autophagy: Unanswered questions. J. Cell Sci. **118:** 7–18.

Klionsky, **D.J.** (2007). Autophagy: From phenomenology to molecular understanding in less than a decade. Nat. Rev. Mol. Cell Biol. **8:** 931–937.

Klionsky, **D.J.**, **and Ohsumi**, **Y.** (1999). Vacuolar import of proteins and organelles from the cytoplasm. Annu. Rev. Cell Dev. Biol. **15:** 1–32.

Kuma, **A.**, **Hatano**, **M.**, **Matsui**, **M.**, **Yamamoto**, **A.**, **Nakaya**, **H.**, **Yoshimori**, **T.**, **Ohsumi**, **Y.**, **Tokuhisa**, **T.**, **and Mizushima**, **N.** (2004). The role of autophagy during the early neonatal starvation period. Nature **432:** 1032–1036.

Lam, **E.** (2004). Controlled cell death, plant survival and development. Nat. Rev. Mol. Cell Biol. **5:** 305–315.

Levine, **B.**, **and Yuan**, **J.** (2005). Autophagy in cell death: An innocent convict? J. Clin. Invest. **115:** 2679–2688.

Liu, **Y.**, **Schiff**, **M.**, **Czymmek**, **K.**, **Tallóczy**, **Z.**, **Levine**, **B.**, **and Dinesh-Kumar**, **S.P.** (2005). Autophagy regulates programmed cell death during the plant innate immune response. Cell **121:** 567–577.

Matile, **P.**, **and Winkenbach**, **F.** (1971). Function of lysosomes and lysosomal enzymes in the senescing corolla of the morning glory (*Ipomoea purpurea*). J. Exp. Bot. **22:** 759–771.

Meijer, **W.H.**, **van der Klei**, **I.J.**, **Veenhuis**, **M.**, **and Kiel**, **J.A.** (2007). ATG genes involved in non-selective autophagy are conserved from yeast to man, but the selective Cvt and pexophagy pathways also require organism-specific genes. Autophagy **3:** 106–116.

Mizushima, **N.** (2005). The pleiotropic role of autophagy: From protein metabolism to bactericide. Cell Death Differ. **12:** 1535–1541.

Morris, **K.**, **MacKerness**, **S.A.**, **Page**, **T.**, **John**, **C.F.**, **Murphy**, **A.M.**, **Carr**, **J.P.**, **and Buchanan-Wollaston**, **V.** (2000). Salicylic acid has a role in regulating gene expression during leaf senescence. Plant J. **23:** 677–685.

Mou, Z., Fan, W., and Dong, X. (2003). Inducers of plant systemic acquired resistance regulate NPR1 function through redox changes. Cell 113: 935–944.

Neuenschwander, U., Vernooij, B., Friedrich, L., Uknes, S., Kessmann, H., and Ryals, J. (1995). Is hydrogen peroxide a second messenger of salicylic acid in systemic acquired resistance? Plant J. 8: 227–233.

Oh, S.A., Park, J.H., Lee, G.I., Paek, K.H., Park, S.K., and Nam, H.G. (1997). Identification of three genetic loci controlling leaf senescence in Arabidopsis thaliana. Plant J. 12: 527–535.

Onodera, J., and Ohsumi, Y. (2005). Autophagy is required for maintenance of amino acid levels and protein synthesis under nitrogen starvation. J. Biol. Chem. 280: 31582–31586.

Overmyer, K., Brosché, M., and Kangasjärvi, J. (2003). Reactive oxygen species and hormonal control of cell death. Trends Plant Sci. 8: 335–342.

Panstruga, R. (2005). Serpentine plant MLO proteins as entry portals for powdery mildew fungi. Biochem. Soc. Trans. 33: 389–392.

Patel, S., and Dinesh-Kumar, S.P. (2008). Arabidopsis ATG6 is required to limit the pathogen-associated cell death response. Autophagy 4: 20–27.

Pattingre, S., Tassa, A., Qu, X., Garuti, R., Liang, X.H., Mizushima, N., Packer, M., Schneider, M.D., and Levine, B. (2005). Bcl-2 antiapoptotic proteins inhibit Beclin 1-dependent autophagy. Cell 122: 927–939.

Phillips, A.R., Suttangkakul, A., and Vierstra, R.D. (2008). The ATG12-conjugating enzyme ATG10 is essential for autophagic vesicle formation in Arabidopsis thaliana. Genetics 178: 1339–1353.

Rose, T.L., Bonneau, L., Der, C., Marty-Mazars, D., and Marty, F. (2006). Starvation-induced expression of autophagy-related genes in Arabidopsis. Biol. Cell 98: 53–67.

Saskia, C.M., and van Wees, J.G. (2003). Loss of non-host resistance of Arabidopsis NahG to Pseudomonas syringae pv. phaseolicola is due to degradation products of salicylic acid. Plant J. 33: 733–742.

Scherz-Shouval, R., Shvets, E., Fass, E., Shorer, H., Gil, L., and Elazar, Z. (2007). Reactive oxygen species are essential for autophagy and specifically regulate the activity of Atg4. EMBO J. 26: 1749–1760.

Shah, J. (2003). The salicylic acid loop in plant defense. Curr. Opin. Plant Biol. 6: 365–371.

Smith, M.T., Saks, Y., and van Staden, J. (1992). Ultrastructural changes in the petals of senescing flowers of Dianthus caryophyllus L. Ann. Bot. (Lond.) 69: 277–285.

Staswick, P.E., Tiryaki, I., and Rowe, M.L. (2002). Jasmonate response locus JAR1 and several related Arabidopsis genes encode enzymes of the firefly luciferase superfamily that show activity on jasmonic, salicylic, and indole-3-acetic acids in an assay for adenylation. Plant Cell 14: 1405–1415.

Surpin, M., Zheng, H., Morita, M.T., Saito, C., Avila, E., Blakeslee, J.J., Bandyopadhyay, A., Kovaleva, V., Carter, D., Murphy, A., Tasaka, M., and Raikhel, N. (2003). The VTI family of SNARE proteins is necessary for plant viability and mediates different protein transport pathways. Plant Cell 15: 2885–2899.

Takahashi, H., Chen, Z., Du, H., Liu, Y., and Klessig, D.F. (1997). Development of necrosis and activation of disease resistance in transgenic tobacco plants with severely reduced catalase levels. Plant J. 11: 993–1005.

Tal, M.C., Sasai, M., Lee, H.K., Yordy, B., Shadel, G.S., and Iwasaki, A. (2009). Absence of autophagy results in reactive oxygen species-dependent amplification of RLR signaling. Proc. Natl. Acad. Sci. USA 106: 2770–2775.

Thompson, A.R., Doelling, J.H., Suttangkakul, A., and Vierstra, R.D. (2005). Autophagic nutrient recycling in Arabidopsis directed by the ATG8 and ATG12 conjugation pathways. Plant Physiol. 138: 2097–2110.

Thordal-Christensen, H., Zhang, Z., Wei, Y., Colloge, D.B., Zhang, Z., Wei, Y., and Colloge, D.B. (1997). Subcellular localization of H_2O_2 in plants. H_2O_2 accumulation in papillae and hypersensitive response during the barley-powdery mildew interaction. Plant J. 11: 1187–1194.

Thumm, M., Egner, R., Koch, B., Schlumpberger, M., Straub, M., Veenhuis, M., and Wolf, D.H. (1994). Isolation of autophagocytosis mutants of Saccharomyces cerevisiae. FEBS Lett. 349: 275–280.

Tsukada, M., and Ohsumi, Y. (1993). Isolation and characterization of autophagy-defective mutants of Saccharomyces cerevisiae. FEBS Lett. 333: 169–174.

van der Graaff, E., Schwacke, R., Schneider, A., Desimone, M., Flugge, U.I., and Kunze, R. (2006). Transcription analysis of Arabidopsis membrane transporters and hormone pathways during developmental and induced leaf senescence. Plant Physiol. 141: 776–792.

van Doorn, W.G., and Woltering, E.J. (2005). Many ways to exit? Cell death categories in plants. Trends Plant Sci. 10: 117–122.

van Doorn, W.G., and Woltering, E.J. (2008). Physiology and molecular biology of petal senescence. J. Exp. Bot. 59: 453–480.

van Wees, S.C., and Glazebrook, J. (2003). Loss of non-host resistance of Arabidopsis NahG to Pseudomonas syringae pv. phaseolicola is due to degradation products of salicylic acid. Plant J. 33: 733–742.

Wada, S., Ishida, H., Izumi, M., Yoshimoto, K., Ohsumi, Y., Mae, T., and Makino, A. (2009). Autophagy plays a role in chloroplast degradation during senescence in individually darkened leaves. Plant Physiol. 149: 885–893.

Wang, D., Amornsiripanitch, N., and Dong, X. (2006). A genomic approach to identify regulatory nodes in the transcriptional network of systemic acquired resistance in plants. PLoS Pathog. 2: 1042–1050.

Wildermuth, M.C., Dewdney, J., Wu, G., and Ausubel, F.M. (2001). Isochorismate synthase is required to synthesize salicylic acid for plant defence. Nature 414: 562–565.

Xie, D.X., Feys, B.F., James, S., Nieto-Rostro, M., and Turner, J.G. (1998). COI1: An Arabidopsis gene required for jasmonate-regulated defense and fertility. Science 280: 1091–1094.

Xiong, Y., Contento, A.L., and Bassham, D.C. (2005). AtATG18a is required for the formation of autophagosomes during nutrient stress and senescence in Arabidopsis thaliana. Plant J. 42: 535–546.

Xiong, Y., Contento, A.L., Nguyen, P.Q., and Bassham, D.C. (2007). Degradation of oxidized proteins by autophagy during oxidative stress in Arabidopsis. Plant Physiol. 143: 291–299.

Yoshimoto, K., Hanaoka, H., Sato, S., Kato, T., Tabata, S., Noda, T., and Ohsumi, Y. (2004). Processing of ATG8s, ubiquitin-like proteins, and their deconjugation by ATG4s are essential for plant autophagy. Plant Cell 16: 2967–2983.

Zhang, Y., Qi, H., Taylor, R., Xu, W., Liu, L.F., and Jin, S. (2007). The role of autophagy in mitochondria maintenance: characterization of mitochondrial functions in autophagy-deficient S. cerevisiae strains. Autophagy 3: 337–346.